International Journal of Thin Films Science and Technology

http://dx.doi.org/10.18576/ijtfst/110101

Characterization of Cobalt Selenide Films using FESEM and EDX

Ho Soonmin[*]

INTI International University, Putra Nilai, 71800, Negeri Sembilan, Malaysia

Received: 21 Jun. 2021, Revised: 2 Sep. 2021, Accepted: 3 Oct. 2021.
Published online: 1 Jan. 2022.

Abstract: Preparation of thin films via chemical and physical deposition technique had been reported by many researchers. The obtained films were characterized by using various tools. Thin films were used in different applications including solar cell, light emitting diode, capacitor, photo detector, ultra violet opto-electronics, and photonic integrated circuit. In this work, the successive ionic layer adsorption and reaction (SILAR) method was used because of low temperature deposition, the simplest and the cheapest deposition method. This is the first time, composition of thin films (under various deposition cycles) was studied using energy dispersive x-ray analysis (EDX). EDX results confirmed that the atomic percentage of cobalt and selenide strongly depended on the number of deposition cycle in the experiment. Larger grain size could be observed for the thin films deposited for 20 cycles based on the field emission scanning electron microscopy analysis.
Keywords: Thin film, SILAR deposition, morphology, cobalt selenide, solar cell, semiconductor.

1 Introduction

Synthesis and characterization of thin films have been reported by many researchers [1-3]. Physical and chemical deposition techniques [4-6] were used to produce binary, ternary, quaternary and pen ternary films. The obtained thin films were characterized by using various tools to investigate the properties of films. For example, structure, electrical, composition, morphology, topography and optical properties were investigated via X-ray diffraction [7], energy dispersive x-ray analysis, scanning electron microscopy, atomic force microscopy [8], UV-visible spectrophotometer [9], Raman spectroscopy, X-ray photoelectron spectroscopy [10], and Fourier transform infrared spectroscopy [11].

In this work, cobalt selenide thin films were deposited onto glass substrate by using successive ionic layer adsorption and reaction under different deposition cycles. Characterization of thin films was carried out via energy dispersive x-ray analysis, and field emission scanning electron microscopy (to study the composition and morphology of samples).

2 Experimental Details

2.1 Preparation of Thin Films

Several chemicals such as cobalt (II) chloride hexahydrate ($CoCl_2.6H_2O$) and sodium selenite (Na_2O_3Se) were employed (without further purification) for the production of films. The microscope glass slide was selected (substrate) in this work. The glass slide was cleaned by acetone, and de-ionized water before use. During the synthesis of films, the glass slide immersed in the 0.25 M cationic solution (Co^{2+} ion) for 25 seconds. After rinsing with de-ionized water for 7 seconds, it was immersed in 0.25 M anionic solution (Se^{2-} ions) for 25 seconds. Then, rinsing with de-ionized water for 7 seconds (to remove the loose material on sample). The pH of reaction solutions was pH=2.3. The sodium hydroxide (NaOH) and hydrochloric acid (HCl) solution were used to adjust the pH value. The films were collected after completed deposition process (10, 15 and 20 cycles), rinsed by de-ionized water, and lastly, place in the oven for 24 hours.

2.2 Characterization of Thin Films

The surface morphologies of the films were investigated by using field emission scanning electron microscope (FEI, Nova Nanosem 230). The presence of different elements in obtained films could be determined by using energy dispersive analysis of the X-ray (EDX) analyzer.

3 Results and Discussions

[*]Corresponding author E-mail: *soonmin.ho@newinti.edu.my*

Generally, thin film deposition methods could be grouped into two categories such as physical technique and chemical method. The successive ionic layer adsorption and reaction (SILAR) method was used for deposition of films. This deposition technique possesses many advantages [12] and can produce film thicknesses in the range of tenths of nanometers to several micrometers [13]. This method consisted of two parts including adsorption of ion onto the substrate and reaction of the adsorbed ion layer will be observed [14]. There are many tools such as AFM, XRD, EDX, SEM, XPS, TEM, STM, UV-visible spectrophotometry, FTIR spectroscopy, and Raman spectroscopy have been used for the characterization of obtained films. Scanning electron microscopy (SEM) and energy dispersive X-ray (EDX) analysis of binary (Table 1), ternary (Table 2) and quaternary thin films (Table 3) were reported by many researchers.

Table 1: Scanning electron microscopy and energy dispersive X-ray analysis of binary thin films.

Thin films	EDX and SEM/FESEM results
ZnSe	EDX: Atomic ratio of Se:Zn =47.88: 46.58 SEM: flower like morphology [15]
ZnSe	EDX: Atomic ratio of Zn:Se =49.44: 50.55 SEM: Crystallite sizes (100-300 nm) thickly packed together [16]
SnSe	EDX: Atomic ratio of Sn:Se =49.7: 50.3 SEM: uniform distribution of grain size, compact and fined grained [17]
SnSe	EDX: Atomic ratio of Sn:Se =48.8: 51.2 SEM: grain size in elongated direction, film thickness was 10 μm [18]
SnSe	EDX: Atomic ratio of Sn:Se =49.93: 50.07 SEM: worm-like grains, grains distributed uniformly could be observed [19]
SnS	EDX: Molar ratio of Sn:S =1:0.96 SEM: grain sizes about 0.2 to 0.5 μm [20]
Cu_2S	EDX: Average atomic ratio of copper:sulfur was 1.89, 1.95 & 2.25 for the films prepared at 55, 65 & 75 °C, respectively. SEM: smaller grain size was observed for the films deposited at lower bath deposition temperature [21]
CuS	EDX: Atomic percentage of Cu:S was 56.87:43.13 for the films deposited at 20 minutes. SEM: Grain size increased with increasing deposition time from 5 to 20 minutes [22].
CdS	EDX: Atomic percentage of cadmium:sulfur was 53.12: 46.88. SEM: Spherical shaped, small grain, homogeneous morphology [23]
CdS	EDX: The obtained films indicated good stoichiometry SEM: The surface is smooth, uniformly covered with nano particles [24].
CdSe	EDX: Atomic percentage of selenium:cadmium is 76.44: 23.56 for the films prepared at room temperature [25]. Atomic percentage of selenium: cadmium is 15.47: 84.53 for the films synthesized at 100 °C. SEM: Grains were polycrystalline and covered entire surface of substrate.
CdTe	EDX: Results indicated Cd-Te ratio is almost stoichiometric [26]. SEM: big grain size, low porosity and uniform coverage in as-deposited films.
CdTe	EDX: The films prepared at cathodic voltage less than 1360 mV showed Te-richness. The films produced at 1360 mV indicated cadmium richness [27]. SEM: Agglomeration of small crystallites, cauliflower-like shaped in as-deposited films.

Table 2: Scanning electron microscopy and energy dispersive X-ray analysis of ternary thin films.

Thin films	EDX and SEM results
$CuInS_2$	EDX: The atomic percentage of copper, indium and sulfur was 35.62:21.6:42.78 when [Cu]/[In]=1.2. SEM: The porous and dense morphology for the films prepared using [Cu]/[In]=0.8, and [Cu]/[In]=1.2, respectively [28].
$CuInS_2$	EDX: atomic percentage of copper:indium:Sulphur was 22%:28%:50% SEM: Film thickness and grain size were 350 nm and 500 nm, for the films prepared using lowest concentration of precursors [29].
$CuInSe_2$	EDX: Cu/In ratio (0.43 to 1.2) and Se/[Cu+In] ratio (0.92 to 1.47) were studied [30]. SEM: The films exhibited big and densely packed crystal morphologies (size= 5 µm)
$CuinSe_2$	EDX: The films consisted of same amount of indium and selenium. However, samples contained more copper when the films were produced at higher temperature and longer deposition time [31]. SEM: the films showed dendritic structure, not-well defined grains, agglomerated and film thickness (90 µm).
$CuInSe_2$	EDX: The films exhibited high selenium content [32]. SEM: Rough surface morphologies, indicating reaction process has not been fully completed for the films prepared at 300 °C.
$CuInSe_2$	EDX: The ratio of copper, indium and selenium about 1:1:2. SEM: Grain size (100 nm) was observed for the films prepared at 400 °C for 1 hour [33].
$CuInSe_2$	EDX: The films showed poor in copper and rich in indium [34]. SEM: Different morphologies could be observed for the films prepared at 550 °C (dense, compact) and 650 °C (laminar morphology with various shapes).
$CuInSe_2$	EDX: Analysis results showed face-to-face annealing providing stoichiometry ratio of (Cu+In)/Se about 1. SEM: Bigger grain size (3 µm) could be observed [35] by applying larger weights (5.2 kg).
$CuInTe_2$	EDX: The films prepared at -0.5 V, -0.6 V, -0.7 V and -0.8 V showed stoichiometry ratio near to $CuInTe_2$. SEM: Polycrystalline was observed [36].

Table 3: Scanning electron microscopy and energy dispersive X-ray analysis of quaternary thin films

Thin films	EDX and SEM results
Cu_2ZnSnS_4	EDX: Zn/Sn values are 0.68%, 0.69%, 0.7% and 0.71% for the films prepared at 1.1V, 1.2V, 1.3V and 1.4 V, respectively. SEM: Uniform thickness [37] without tiny holes could be observed for the films deposited at 1.4 V.
Cu_2ZnSnS_4	EDX: The presence of copper, zinc, sulfur and tin in sample could be detected [38]. SEM: larger grains could be seen in high temperature treatment films.
Cu_2ZnSnS_4	EDX: The film prepared at 450 °C, 60 minutes, indicated Zn/Sn, Cu/[Zn+Sn] and S/metal ratio were 0.87, 1.48 and 0.8, respectively [39]. SEM: Uniform, dense without voids could be seen in samples.

Cu_2ZnSnS_4	EDX: Atomic percentage values of copper: zinc: tin: sulphur were in the range 22.82 to 29.51: 19.88 to 28.82: 9.62 to 12.81: 37.8 to 38.74 for the films prepared onto soda lime glass [40]. EDX: Atomic percentage values of copper: zinc: tin: sulphur were in the range 25.58 to 30.51: 18.61 to 28.52: 11.26 to 12.73: 34.64 to 39.42 for the films prepared onto ITO glass. SEM: The most homogeneous surface was observed in ITO substrate. Inhomogeneous grains with porosity could be seen in soda lime glass.
Cu_2ZnSnS_4	EDX: Atomic percentage of copper: zinc: tin: Sulphur was 22.95: 11.38: 12.51: 53.16 in the obtained sample [41]. SEM: Smooth, compact and uniform morphology with size (1 µm) was observed for the films prepared at 580 °C.
Cu_2ZnSnS_4	EDX: Copper richcomposition, zinc and tin loss in annealed sample under flow rate of gas more than 60 sccm [42]. SEM: The films showed dense and polycrystalline structure
Cu_2ZnSnS_4	EDX: Copper poor and zinc rich composition were observed for the films prepared at deposition potential from -0.85 V to -1.05 V SEM: Formation of interconnected grains, and an increase in grain size could be seen [43]
Cu_2ZnSnS_4	EDX: the atomic percentage of copper:zinc: tin: Sulphur was 36.64:16.26:23.11:25.99. SEM: The obtained samples showed uniform size (less than 100 nm), smooth and homogeneous [44].
Cu_2ZnSnS_4	EDX: As-deposited films indicated composition close to stoichiometric. The loss of tin could be observed in annealed samples [45]. SEM: Lateral grain and columnar in shape could be seen in as-deposited films and annealed samples.

The energy dispersive X-ray (EDX) analysis is used in different research areas such as biomedical fields, environmental pollution, engineering and material science. It is very useful tool to study nanoparticles, to investigate heavy metals pollutions, to determine the composition of samples, and showed high sensitivity in detecting the various elements in tissues [46]. Generally, it is a technique of elemental analysis associated to electron microscopy based on the generation of characteristic X-rays that reveals the presence of elements present in the samples [47]. The scanning electron microscopy (SEM) was used in various types of science and industry applications. This is due to

SEM produced high resolution, sharp, black and white images [48]. Several advantages were highlighted by researcher such as easy to operate, samples required minimal preparation actions, and it works fast [49]. Basically, SEM can focused electron beam over a surface to create picture. The electrons in the beam interact with the sample, forming different signals, could be employed to obtain information (surface topography and composition). Table 4 showed some limitations of transmission electron microscopy (TEM), atomic force microscopy (AFM) and scanning tunneling microscope (STM).

Table 4: Limitation of TEM, AFM and STM.

Transmission Electron Microscopy (TEM)	atomic force microscopy (AFM)	scanning tunneling microscope (STM)
It is very large [50]and very expensive	Maximum scanning area is 150 x150 µm [52]	It is very expensive and could be very difficult to use effectively [54]
It required special housing [51] and maintenance	Image a maximum height on the order of 10-20 µm [53]	Required a lot of skill to operate it [55]

The compositional analysis of the obtained films was studied by using the energy dispersive analysis (EDX) of the X-ray technique. The EDX spectrum of the cobalt

selenide thin films deposited under 10 cycles as shown in figure 1a. The quantitative elemental analysis was done only for the selenium and cobalt. The atomic percentage (%) for cobalt and selenium was 53.52 % and 46.48%, respectively. When the films deposited for 15 cycles, the atomic percentage for selenium and cobalt was 72.99% and 27.01% respectively (figure 1b). Lastly, the films prepared deposited under 20 cycles (figure 1c) showed the atomic percentage for cobalt and selenium was 39.73% and 60.27%. From the EDX analysis studies, the amount of cobalt and selenium strongly depended on the number of deposition cycle during the experiment. Veeradasan and co-workers [56] reported that EDX spectra of the zinc oxide films with different Au thicknesses. Hend and co-workers [57] highlighted that the presence of zinc and oxygen with a pure phase in obtained samples based on EDX spectra.

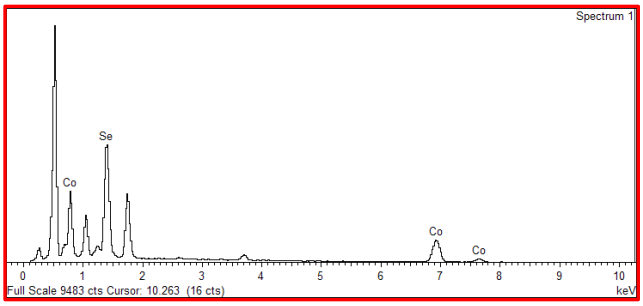

[a]

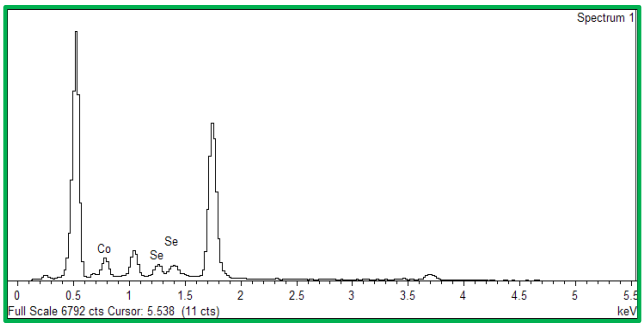

[b]

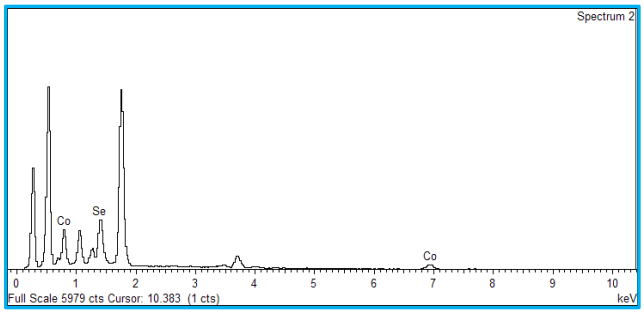

[c]

Fig.1: EDX spectrum for the cobalt selenide films deposited under [a] 10 cycles [b] 15 cycles [c] 20 cycles.

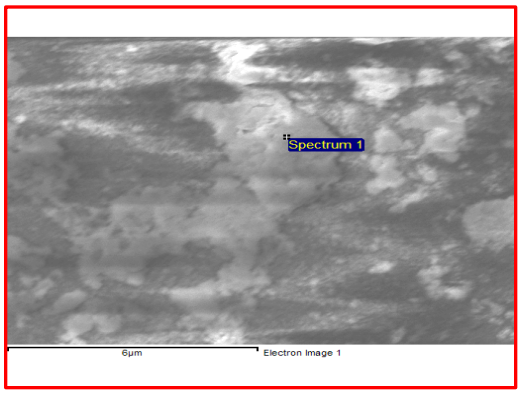

[a]

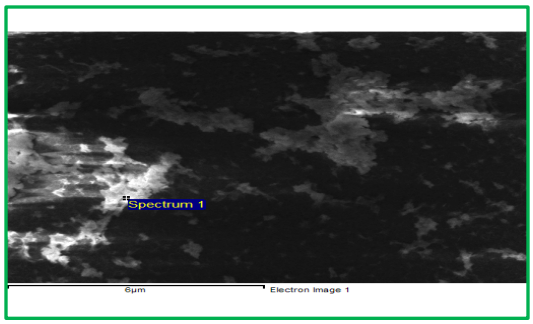

[b]

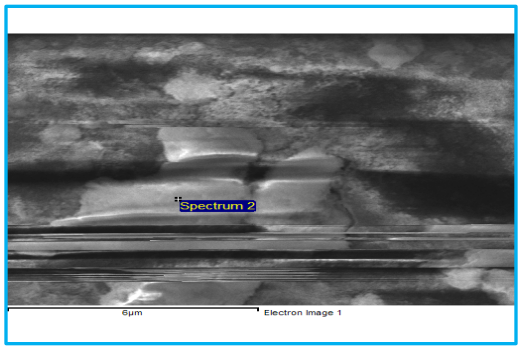

[c]

Fig.2: FESEM images for the cobalt selenide films deposited under [a] 10 cycles [b] 15 cycles [c] 20 cycles.

The films prepared using 10 (figure 2a) and 15 (figure 2b) deposition cycles indicated smaller grain size (0.5 to 1 µm). FESEM images exhibited inhomogeneous morphology and the grains partially covered the surface of the substrate. Researchers pointed out that large pinhole sizes caused poor device performance [58] in solar cell applications. This is because of a large number of trap assisted recombination centers of trapping and lower carrier mobilities [59]. On the other hand, the films deposited under 20 deposition cycles (figure 2c) showed bigger grain (1-2 µm). FESEM analysis confirmed that the grains covered entire surface of substrate. Scientists concluded that bigger grain will

improve the performance of the solar cell [60], because of the charge carriers encounter fewer trapping [61] and scattering sources [62].

4 Conclusions

The cobalt selenide thin films were produced onto soda lime glass via SILAR method under various deposition cycles. The morphology and composition of obtained films were studied by using FESEM and EDX. Experimental findings highlighted that deposition cycles played an important role in the formation of the films as indicated in the EDX spectra. FESEM showed that the grain size increases as the SILAR deposition cycle was increased from 10 to 20 cycles.

Acknowledgements

Research work funded by INTI International University (INTI Internal Research Grant INTI –CAE-01-01-2018).

References

[1] P. Sylwia, D. Pociecha, J. Maria, and L. Wiktor. Thermomechanically controlled fluoresnce anisotropy in tghin films of InP/ZnS quantum dots, *Nanoscale Adv*., DOI: 10.1039/D1NA00290B, (2021).

[2] R. Khatri, and J. Patel. Thickness dependent studies of chemically grown transparent conducting Cu:ZnS thin films for optoelectronic applications, *Opt. Mater*., https://doi.org/10.1016/j.optmat.2021.111469 (2021).

[3] A. Jesu, R. Ade, D. Naidu, and V. Ganesh. Optical manipulation of nebulizer spray pyrolysed ZnS thin films for photodetector appliactions: effect of Al, Sn and Sb doping, *Opt. Mater.,* https://doi.org/10.1016/j.optmat.2021.111177 (2021).

[4] M. Harif, S. Rahman, H. Rosly, M. Isah, and N. Amin. Microstrutural evolution of oxygen incorporated CdTe thin films deposited by closed spaced sublimation, *Mater. Lett.,* https://doi.org/10.1016/j.matlet.2021.130552 (2021).

[5] M. Taj, M. Farhan, M. Arshad, and A. Shah. Synthesis of thermally evaporated ZnSe thin film at room temperature, *Thin Solid Films*, **519,** 5971-5977 (2011).

[6] S.M. Ho. Chemical bath deposited lead sulphide thin films: Preparation and characterization, *World Mech*., **1,** 1-6 (2014).

[7] S. Atan, K. Anuar, S.M. Ho, W. Tan, and N. Saravanan. Effect of deposition period and pH on chemical bath deposited Cu_4SnS_4 thin films, *Philipp. J. Sci*., **138,** 161-168 (2009).

[8] S.M. Ho. Chalcogenide thin films prepared using chemical bath deposition method: Review, *Res. J. Appl. Sci. Eng. Technol*., **11**, 1058-1065 (2015).

[9] S. Gangawane, P. Malekar, and V. Fulari. Effect of electron irradiation on the crystallite size, grain size and band gap energy of electrodepoisted cadmium sulfide thin films, *Mater. Today Proc*., https://doi.org/10.1016/j.matpr.2021.05.272 (2021).

[10] W. Mohd, H. Nakajima, N. Chanlek, F. Yap, and N. Azah. X-ray photoelectron spectroscopy analysis of chitosan graphene oxide based composite thin films for potential optical sensing application, *Polymers,* https://doi.org/10.3390/polym13030478 (2021).

[11] M. Abdelghany, M. Awad, and S. Meikhail. Electrical conductivity of chitosan/PCL hosting network for CdSe quantum dots, *Polymer Bull*., https://doi.org/10.1007/s00289-021-03715-9 (2021).

[12] A. Taser, M. Emin, and H. Guney. Fe doping effects in MgO thin films grown with SILAR technique, *Mater. Chem. Phys.,* https://doi.org/10.1016/j.matchemphys.2021.124993 (2021).

[13] T. Das, S. Vinoth, H. Hegazy, and M. Shkir. Optoelectronic proeprties of CuO thin films fabricated by facile SILAR dip coating technique for photosensing applications, *J. Inorg. Organomet. Polym. Mater.,* https://doi.org/10.1007/s10904-021-01928-z (2021).

[14] S. Prabath, C. Elena, J. Ren, and G. Massimo. SILAR deposition of metal oxide nanostructured films, *Nano Micro Small*, https://doi.org/10.1002/smll.202101666 (2021).

[15] G. Bakiyaraj, and R. Dhanasekaran. Synthesis and characterization of flower-like ZnSe nanostructured thin films by chemical bath deposition (CBD) method, *Appl. Nanosci.,* **3**, 125-131 (2013).

[16] A. Yousef. Composition and band gap controlled AACVD of ZnSe and ZnS_xSe1_{-x} thin films using novel single source precursors, *Mater. Sci. Appl.,* 10.4236/msa.2017.810052 (2017).

[17] R. Mariappan, M. Ragavendar, and G. Gowrisankar. Growth and characterization of SnSe thin films prepared by spray pyrolysis technique, *Chalcogen. Lett*., **7**, 211-216 (2010).

[18] H. Yanuar, U. Lazuardi, and J. Copriady. Preparation and characterization of thin film SnSe used by close spaced vapor transport technique, *Chalcogen. Lett.,* **14**, 181-185 (2017).

[19] G. Kunjomana, B. John, and R. Karthikeyan. Processing and characterization of tin chalcogenide thin films by thermal evaporation, *Int. J. Curr. Res. Rev*., **10,** 46-48 (2018).

[20] H. Ariswan, and R. Prasetyawati. Crystal Structure, optical, and electrical properties of SnSe and SnS semiconductor thin films prepared by vacuum evaporation techniques for solar cell applications, *IOP Conf. Ser. Mater. Sci. Eng.,* doi:10.1088/1757-899X/202/1/012042 (2017).

[21] K. Anuar, S.M. Ho, K.S. Lim, and N. Saravanan. SEM, EDAX and UV-visible studies on the properties of Cu_2S thin films, *Chalcogen. Lett.,* **8,** 405-410 (2011).

[22] S. Dhasade, S. Patil, and V. Fulari. Studies on synthesis and characterization of copper sulfide thin films, *J. Shivaji Univ. Sci. Technol.*, **41**, 1-3 (2014).

[23] S. Navale, T. Mane, M. Shinde, J. Kim, and B. Patil. Highly selective and sensitive CdS thinfilm sensorsfor detection of NO_2 gas. *RSC Adv.,* https://doi.org/10.1039/C4RA06531J (2014).

[24] C. Tarun, D. Kumar, M. Zaman, and P. Rajaram. Structural, optical and photoelectric properties of sprayed CdS thin films, *AIP Conf. Proc*., https://doi.org/10.1063/1.5033003 (2018).

[25] B. Sahuban, S. Kumar, K. Sri, and A. Ayeshamariam. Effect of temperature of electron beam evaporated CdSe thin films, *J. Mater. Sci. Eng.,* DOI: 10.4172/2169-0022.1000297 (2016).

[26] M. Nikale, S. Shinde, H. Bhosale, and Y. Rajpure. Physical properties of spray deposited CdTe thin films: PEC performance, *J. Semicond*., https://doi.org/10.1088/1674-4926/32/3/033001 (2011).

[27] A. Ojo, and M. Dharmadasa. Analysis of electrodeposited CdTe thin films grown using cadmium chloride precursor for applications in solar cells, *J. Mater. Sci. Mater. Electron*., **28**, 14110-14120 (2017).

[28] B. Mazabalo, K. Napo, S. Koffi, D. Mani, and D. Soro. Role of [Cu]/[In] Molar Ratio in Controlling Structural, Morphological and Optical Properties of Sprayed $CuInS_2$ Thin Films, *Adv. Mater.,* **7**, 111-117 (2018).

[29] F. Anna, S. Angela, T. Bein, and C. Scheu. A biomolecule-assisted, cost-efficient route for growing tunable $CuInS_2$ films for green energy application, *RSC Adv.,* **7**, 20219-20230 (2017).

[30] F. Adurodija, K. Yoon, J. Song, S. Kim, and T. Ahn. Preparation of $CuInSe_2$ thin films by selenization of co-sputtered Cu–In precursors, *J. Mater. Sci. Mater. Electron*., **9**, 361-366 (1998).

[31] I. Algimantas, A. Ingrida, and I. Remigijus. Effect of In-Incorporation and Annealing on Cu_xSe Thin Films, Materials, https://doi.org/10.3390/ma14143810 (2021).

[32] P. Zaretskaya, V. Zalesski, V. Ermakov, and K. Bente. Raman spectroscopy of $CuInSe_2$ thin films prepared by selenization, *J. Phys. Chem. Solids*, **64**, 1989–1993 (2003).

[33] P. Jong, S. Kim, J. Park, M. Kang, and W. Shim. Deposition of $CuInSe_2$ thin films using stable copper and indium selenide precursors through two stage MOCVD method, *Bull. Korean Chem. Soc.,* **30**, 853-856 (2009).

[34] J. Montes, A. Acevedo, R. Correa, and P. Mora. Characterization of $CuInSe_2$ thin films obtained by RF magnetron co-sputtering from CuSe and In targets, Chalcogen. Lett., **13**, 381-388 (2016).

[35] S. Matthias, S. Philipp, L. Graf, and J. Peter. Processing and Characterization of Vacuum-Free $CuInSe_2$ Thin Films from Nanoparticle-Precursors using Novel Temperature Treatment Techniques, *Int. J. Nanoparticle Res*., **2**, 1-10 (2018).

[36] G. Keser, A. Peksoz. Electrochemically growth and characterization of $CuInTe_2$ chalcopyrite thin films, *J. Mater. Sci. Mater. Electron.,* **31**, 15565-15574 (2020).

[37] M. Rao, and S. Basha. Structural and electrical properties of CZTS thin films by electrodeposition, *Results Phys*., **9**, 996-1006 (2018).

[38] M. Mkawi, K. Ibrahim, M. Ali, and M. Salhin. Synthesized and characterization of Cu_2ZnSnS_4 (CZTS) thin films deposited by electrodeposition method, *Appl. Mech. Mater.,* **343**, 85-89 (2013).

[39] D. Xia, Y. Zheng, P. Lei, and X. Zhao. Characterization of Cu_2ZnSnS_4 thin films prepared by solution-based deposition techniques, *Phys. Proc*., **48**, 228–234 (2013).

[40] M. Putut, P. Darma, S. Triastuti, A. Nurul, and K. Rosi. Study of CZTS morphology grown by immersion and sulfurization, *AIP Conf. Proc.,* https://doi.org/10.1063/5.0037824 (2021).

[41] L. Qian, C. Yaru, W. Juan, H. Yu, and S. Tong. Study on the optimization of Cu-Zn-Sn-O to prepare Cu_2ZnSnS_4 thin film via a nano ink coating method, *Front. Chem*., doi: 10.3389/fchem.2021.675642 (2021).

[42] M. Olgar, R. Zan, and S. Erkan. Fabrication of Cu-rich CZTS thin films by two-stage process: Effect of gas flow-rate in sulfurization process, *J. Mol. Struct.,* https://doi.org/10.1016/j.molstruc.2021.129922 (2021).

[43] B. Haribhau, A. Bhorde, and W. Ashish. Single step electrochemical deposition of CZTS thin films with enhanced photoactivity, *ES Mater. Manuf*., DOI: 10.30919/esmm5f934 (2021).

[44] N. Siti, N. Nayan, Z. Azman, R. Saidur, and S. Fhong. Single-phase CZTS thin film prepared by high power impulse magnetron sputtering (HiPIMS): A first attempt, *Int. J. Nanoelectron. Mater.,* **14**, 195-208 (2021).

[45] M. Nowell, M. Oo, L. Johnson, and M. Scarpulla. Grain Size and Texture of Cu_2ZnSnS_4 Thin Films Synthesized by Cosputtering Binary Sulfides and Annealing: Effects of Processing Conditions and Sodium, J. Electron. Mater., https://doi.org/10.1007/s11664-011-1729-3 (2011).

[46] S. Manuel, B. Simone, L. Kaur, and B. Elena. Energy Dispersive X-ray (EDX) microanalysis: A powerful tool in biomedical research and diagnosis, Eur. J. Histochem., doi: 10.4081/ejh.2018.2841 (2018).

[47] S.M. Ho. Application of Energy Dispersive X-Ray Analysis Technique in Chalcogenide Metal Thin Films: Review, *Middle-East J. Sci. Res*., **24**, 445-449 (2016).

[48] W. Zhou, R. Apkarian, Z. Wang, and D. Joy. *Fundamentals of Scanning Electron Microscopy (SEM),* in Scanning Microscopy for Nanotechnology. W. Zhou, Z. Wang. Springer, New York, 1-50, (2006).

[49] L. Reimer. *Scanning electron microscopy: physics of image formation and microanalysis*, 2nd, Springer: Berlin, 13-56, (2000).

[50] B. David, and C. Barry. *Transmission Electron Microscopy: A Textbook for Materials Science*. Springer Science & Business Media, Berlin, 110-119,. (2013).

[51] R. Ludwig, and H. Kohl. *Transmission Electron Microscopy: Physics of Image Formation.* Springer Science & Business Media, Berlin, 1-5, (2008).

[52] M. Bray, H. Cohen, and L. Marcia. *Atomic Force Microscopy/Scanning Tunneling Microscopy*. Springer, New York, 100-110, (2013).

[53] V. Bert. *Scanning Probe Microscopy: Atomic Force Microscopy and Scanning Tunneling Microscopy*. Springer, New York, 140-160, (2015).

[54] W. Roland, and R. Wiesendanger. *Scanning Probe Microscopy and Spectroscopy: Methods and Applications*. Cambridge University Press, United Kingdom, 150-199, (1994).

[55] A. Joseph, and W. Kaiser. *Scanning Tunneling Microscopy.* Academic Press, New York, 1-30, (2013).

[56] P. Veeradasan, H. Uda, R. Ruslinda, and G. Subash. Thickness dependent nano structural, moprhological, optical and impedometric analyses of zinc oxide gold hybrids: nano particle to thin film, *PLOS ONE*, https://doi.org/10.1371/journal.pone.0144964 (2015).

[57] M. Hend, A. Sabry, and M. Mona. Statistical optimization of experimental parameters for extracellular synthesis of zinc oxide nanoparticles by a novel haloalaliphilic Alkalibacillus sp. W7, *Sci. Rep*., https://doi.org/10.1038/s41598-021-90408-y (2021).

[58] G. Dawit, N. Riad, I. Ka, and M. Asuo. Solvent-Antisolvent Ambient Processed Large Grain Size Perovskite Thin Films for High-Performance Solar Cells, *Sci. Rep*., https://doi.org/10.1038/s41598-018-31184-0 (2018).

[59] Z. Liang, S. Zhang, X. Xu, N. Wang, and J. Wang. Large grain size perovskite thin film with a dense structure for planar heterojunction solar cells via spray deposition under ambient conditions, *RSC Adv*., **5**, 60562-60569 (2015).

[60] C. Bo, M. Yang, X. Zheng, W. Li, K. Zhu, and S. Priya. Impact of Capacitive Effect and Ion Migration on the Hysteretic Behavior of Perovskite Solar Cells, *J. Phys. Chem. Lett.,* **6**, 4693-4700 (2015).

[61] Z. Yong, L. Tan, Q. Fu, T. Ji, and Y. Chen. Enhancing the grain size of organic halide perovskites by sulfonate-carbon nanotube incorporation in high performance perovskite solar cells, *Chem. Commun.,* https://doi.org/10.1039/C6CC00268D (2016).

[62] W. Nie, H. Tsai, A. Reza, G. Gupta, and J. Amanda. High-efficiency solution-processed perovskite solar cells with millimeter-scale grains, Science, DOI: 10.1126/science.aaa0472 (2015).